STRUCTURE, PHASE COMPOSITION AND HARDNESS OF TiZrAlN FILMS WITH DIFFERENT Al CONTENT

V.V. Uglov[1)], I.A. Saladukhin[1)], G. Abadias[2)], A.Yu. Daniliuk[1)], S.V. Zlotski[1)], S.N. Dub[3)]
[1)]*Belarusian State University, 4 Nezavisimosti ave., 220030 Minsk, Belarus*
[2)]*Université de Poitiers, SP2MI, Téléport 2, F86962 Chasseneuil-Futuroscope cedex, France*
[3)]*Institute for Superhard Materials, NAS of Ukraine, 04074 Kiev, Ukraine*

Quaternary TiZrAlN films were grown at T_s=600°C by reactive magnetron sputtering in Ar+N_2 plasma discharge from elemental targets. Deposition occurred at the constant power of Ti and Zr targets, while changing the Al power and adjusting the N_2 flow rate, resulting in stoichiometric nitride films (N concentration ~ 50 at.%) with Al content up to 37 at.% and fixed Zr:Ti ratio of 1:1. It is shown that single-phase, cubic $(Ti,Zr)_{1-x}Al_xN$ solid solutions are stabilized upon incorporation of Al. The lattice parameter of Al-containing films linearly decreases with the increase in Al concentration. For these films the maximum hardness (25 GPa) is achieved at Al content of 19 at.%.

Introduction

Protective coatings based on the transition metal (TM) nitrides are related to a class of materials with the unique combination of the properties such as high hardness, high melting point and oxidation resistance that makes them to be attractive in many technological applications [1-3]. Among TM nitrides, the films based on TiN, ZrN and TiZrN are the most widespread [2-3]. The study of Ti-Zr-N nitride is under a great interest [4]. So, the increased hardness of (Ti,Zr)N coatings is the result of the solid solution strengthening mechanism consisting in creation of energy barrier to the movement of dislocations throughout the crystallites which have the distortion of their lattice due to Ti and Zr atomic radius mismatch [4].

In order to improve the properties further, much attention is currently paid to TM systems with the addition of aluminum, in particular, to TiAlN films. TM-Al-N systems, where Al substitutes for TM atoms at the crystal lattice, possess the improved mechanical and thermal properties [5]. The crystal structure and properties of TM-Al-N films are strongly determined by Al content [6]. While keeping the cubic lattice, Al content rise leads to improvement of the mechanical characteristics of TM-Al-N coatings; and they become worse when Al content exceeds its maximum solubility in the cubic phase that is accompanied by the mixed (cubic-NaCl and wurtzite-ZnS) structure formation [6]. Also the incorporation of Al atoms into TiN structure has an effect on the grain growth. At the low Al content, a round columnar growth takes place like in the case of TiN film synthesis. If the aluminum content increases, the film structure becomes more dense (typical 'zone-T' structure is formed which is characterized by much finer grain size and by the mixture of rounded and faceted columns) [5].

Thus, the properties of ternary TM nitride films are closely related to certain characteristics such as atomic content of the constituent elements, phase composition and structure which in turn depend on deposition parameters. At the same time, up to date there are no enough data for investigation of Al incorporation into TiZrN films. That is why the purpose of the present work is a study of the phase composition, growth kinetics, mechanical properties of TiZrAlN films with different atomic composition.

Experimental details

TiZrAlN thin films were deposited on (001) Si wafer covered with native SiO_2 (~2 nm thick) layer using reactive unbalanced magnetron co-sputtering from elemental targets under Ar+N_2 plasma discharges [7]. Deposition was carried out at the substrate temperatures T_s = 600°C in a high vacuum chamber (base pressure ~10^{-5} Pa). Prior to deposition, all targets were sputter-cleaned for 3 min in pure Ar plasma discharge, while the substrate was shielded by a shutter. The Al content, *x*, in the films was varied by changing the RF power supply of the Al target, from 0 up to 300 W, while maintaining the DC power supply of Ti and Zr targets constant (250 and 200 W, respectively). The N_2 flow was varied from 1.1 to 2.1 sccm. This corresponds to N_2 partial pressure in the range of $(8.3–16)\cdot10^{-3}$ Pa, as measured using MKS MicroVisionPlus mass spectrometer. The film thickness was 450-940 nm.

The elemental composition of the as-deposited TiZrAlN films was determined using wavelength dispersive X-ray spectrometry (WDS) and Rutherford backscattering (RBS). WDS was carried out using an Oxford Instruments spectrometer unit attached to a JEOL 7001F-TTLS scanning electron microscope. RBS was performed with 2.0 MeV He^+ ions at the High Voltage Engineering tandetron system accelerator.

XRD analysis was employed for structural identification using a D8 Bruker AXS X-ray diffractometer operating in Bragg–Brentano configuration and equipped with $Cu_{K\alpha}$ wavelength (0.15418 nm) and a scintillation detector.

Cross-sectional TEM specimens have been prepared using an FEI Helios Nanolab 650 FIB. The specimens were analyzed by using a JEOL JEM 2100 LaB6 transmission electron microscope operating at 200 kV.

The hardness and elastic modulus of the films were studied by nanoindentation using a Nano Indenter-G200 system (Agilent Technologies, USA) equipped with a continuous stiffness measurement attachment option (for more details, see Ref. [7]).

Results and discussion

The results of elemental analysis of $(Ti, Zr)_{1-x}Al_xN$ films formed at the different deposition parameters are given in Fig.1.

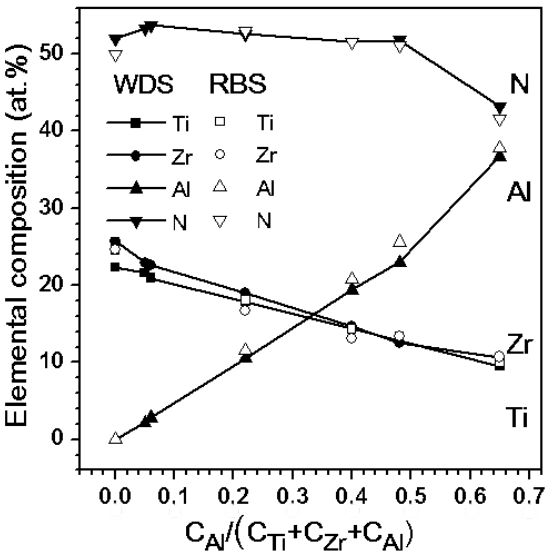

Fig. 1. Elemental composition of TiZrAlN films with different Al/(Ti+Zr+Al) concentration ratio, x

The ratio of powers at Zr and Ti targets was adjusted so that the Zr:Ti concentration ratio in resulting films was close to unit. It was shown earlier [7] that ternary TiZrN films possessed the improved physical and mechanical properties just at such ratio of metal components. For comparative description of the structural-phase state and properties of the films, not Al concentration in atomic percent but the value *x*, which equal to ratio of Al concentration to total concentration of Ti, Zr and Al, was used at the present study.

It follows from the analysis of the data presented in Fig. 1 that *x* increases in proportion to the power at the corresponding Al target. It means that it is possible to reach the necessary content of the incorporated element in the film composition by change of power at Al target. At the same time, Zr:Ti concentration ratio for all $(Ti, Zr)_{1-x}Al_xN$ films remains within 1.0-1.1.

However, in view of an existence of the equipment limits for increase in the power at each of targets in magnetron sputtering process, for further increase in Al content in the film it is necessary to reduce the power at Ti and Zr targets down to 200 and 160 W, respectively (Fig. 1, the sample with x = 0.65).

The nitrogen content in the composition of the films based on TM nitrides has a great influence on their structure and properties [2]. Stoichiometric composition for fcc-structure (NaCl type in the case of TiZrN film) corresponds to nitrogen content of 50 at.%. As it was revealed for quaternary TiZrAlN films [7, 8], if to maintain a nitrogen flow into the chamber at the same rate as at deposition of TiZrN films then at the increase of power at the third target an appreciable reduction of nitrogen content in the films occurs (down to the level lower than 30 at.%). Therefore, it is necessary to take into consideration an effect of higher desorption rate of N_2 dimers on the growing surface at the higher total power under conditions of three targets co-sputtering during film deposition. For this purpose at the present study, when increasing in power at Al target, the value of N_2 flow was adjusted to ensure the stoichiometric content of nitrogen in the resulting films. So, it is necessary to increase N_2 flow from 1.1 (TiZrN film) up to 2.1 sccm ($(Ti, Zr)_{0.52}Al_{0.48}N$ film) with the rise in Al content to keep the nitrogen concentration about 50 at.%.

Thus, $(Ti, Zr)_{1-x}Al_xN$ films with different x and near-stoichiometric nitrogen content were deposited by reactive magnetron sputtering technique when varying Al target power and nitrogen flow into the chamber.

The phase composition of the coatings was analyzed by the XRD method for the reflection angle range 2θ from 20 to 65°. Fragments of XRD patterns for $(Ti, Zr)_{1-x}Al_xN$ films are given in Fig. 2. We have confined the spectra by the angle range 30-44° because beyond of this interval no any additional peaks were registered.

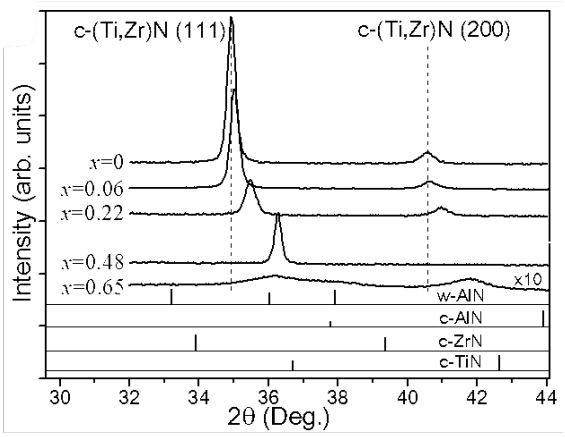

Fig. 2. XRD patterns of $(Ti,Zr)_{1-x}Al_xN$ films with different Al content, x. Patterns corresponding to wurtzite w-AlN (JCPDS card no. 25-1133), cubic c-AlN (JCPDS card no. 25-1495), c-TiN (JCPDS card no. 38-1420) and c-ZrN (JCPDS card no. 35-753) are shown at the bottom

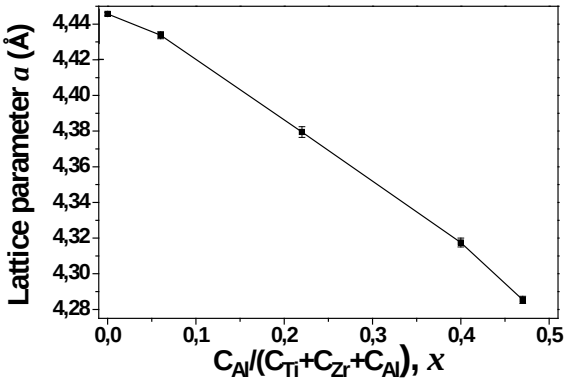

Fig. 3. Lattice parameter, a, of c-(Ti, Zr, Al)N solid solution for $(Ti, Zr)_{1-x}Al_xN$ films as a function of Al content, x

As Fig. 2 indicates, the (111) and (200) peaks of (Ti, Zr)N solid solutions for pure TiZrN film (*x* = 0) are between the corresponding peaks of TiN and ZrN phases which possess by fcc-structure. The (111) preferred orientation is clear for TiZrN film that can be a precondition for high hardness since <111> is the more close-packed plane in TM nitride [4]. When incorporating Al (i.e. with x rise) there is a shift of solid solution peaks to the region of higher angles

that points to reduction of its lattice parameter, a (Fig. 3).

Incorporation of Al with the smaller atomic radius (1.18 Å – for Al, 1.76 Å – for Ti, 2.06 Å – for Zr) results in linear decrease in lattice parameter of c-(Ti, Zr, Al)N solid solution. Dependence of *a* on *x* is close to the linear (Fig. 3). If to approximate it to the case *x* = 1, the obtained value will 4.10 Å that corresponds to the calculated value of the lattice parameter for pure c-AlN [8]. Adduced arguments allows to infer that the structure of $(Ti, Zr)_{1-x}Al_xN$ films is the c-(Ti, Zr, Al)N substitution solid solution for all Al contents which were considered (up to x = 0.65) (Fig. 2).

Only at the maximum Al content in $(Ti, Zr)_{1-x}Al_xN$ film (x = 0.65), the weak reflex in the region $2\theta = 38°$ is registered besides peaks of solid solution (Fig. 2) that can be attributed both to $(10\bar{1}1)$ peak of w-AlN hexagonal phase and to (111) peak of c-AlN cubic phase. As it was shown earlier [8], at lower temperatures of film deposition (T_s=270°C, unlike T_s=600°C used at the present work) the presence of w-AlN hexagonal phase in TiZrAlN film composition was already determined at the concentration ratio $C_{Al} / (C_{Ti}+C_{Zr}+C_{Al}) \geq 0.11$. The films were characterized as the nanocomposites consisting of the grains of c-(Ti, Zr, Al)N solid solution embedded into a highly-disordered 'matrix' phase of aluminum nitride. In our case, it is possible to assume that when reaching x = 0.65 the w-AlN phase appears in $(Ti,Zr)_{1-x}Al_xN$ films also. Formation of this grain-boundary phase promotes hindering of grains growth of c-(Ti, Zr, Al)N solid solution that leads to its peaks intensity reduction (Fig. 2). The similar situation was observed in the previous findings [7, 8].

As it follows from Fig. 4, the TiZrN film is characterized by the column growth structure that is in accordance with the reference data [2, 4]. Column growth remains at the incorporation of Al up to *x* = 0.48 when the single-phase structure on the basis of c-(Ti, Zr, Al)N solid solution is still inherent for $(Ti, Zr)_{1-x}Al_xN$ films (Fig. 4).

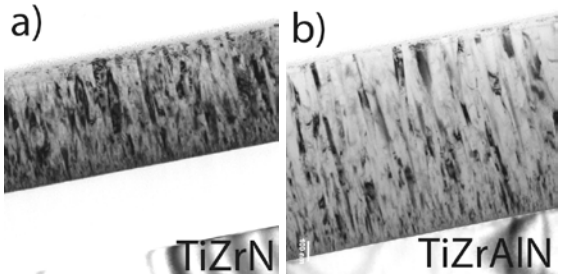

Fig. 4. Cross-sectional TEM of TiZrN film (a) and $(Ti, Zr)_{1-x}Al_xN$ film with x = 0.48 (b)

As it was noted, the incorporation of an additional component into ternary nitride systems at its quite defined concentration can provide the improvement of the mechanical properties of the films [1, 7]. Ascertainment of the possibility of the mechanical properties optimization by means of Al adding to TiZrN film was one of the goals of the present work.

Values of the hardness and Young's modulus for as-deposited $(Ti, Zr)_{1-x}Al_xN$ films are given in Fig 5. One can conclude that the aluminum incorporation in TiZrN composition does not essentially influence on the hardness of the films. The maximum hardness is achieved at Al content of 19 at.% (x = 0.40 in $(Ti, Zr)_{1-x}Al_xN$ composition) and it is equal to 25 GPa.

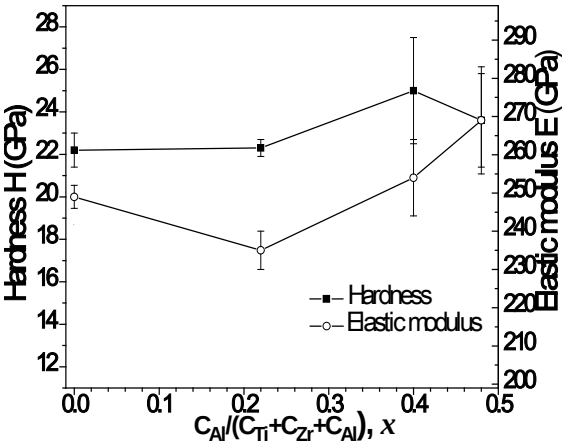

Fig. 5. Hardness, H, and elastic modulus, E, for TiZrN and $(Ti,Zr)_{1-x}Al_xN$ films with different Al content, *x*.

Conclusion

Quaternary TiZrAlN films with different Al content were synthesized by simultaneous reactive magnetron sputtering of Ti, Zr and Al targets under $Ar+N_2$ plasma discharges. By means of variation of N_2 flow into the camera, the films deposition regimes were optimized to provide near stoichiometric content of nitrogen in their structure.

The features of the phase composition and structure formation of TiZrN films at the incorporation of Al were ascertained. The c-(Ti, Zr, Al)N solid solution of substitution type is the basis of $(Ti, Zr)_{1-x}Al_xN$ ($0.05 \leq x \leq 0.65$) system and the films are characterized by the column structure of growth.

At the defined ratio of the components, the increase in hardness of the quaternary TiZrAlN films is achieved. The maximum hardness (25 GPa) is observed at Al concentration of 19 at.%.

References

1. *Veprek S., Veprek-Heijman M., Karvankova P. et al.* // Thin Solid Films. 2005. V. 476. P. 1–29.
2. *Constantin D.G., Munteanu D.* // Series I: Engineering Sciences 5 (54). 2012. № 2. P. 59–64.
3. *Roman D., de Amorim C., de Souza F., et al.* // Materials Chemistry and Physics. 2011. V.130. P. 147–153.
4. *Lin Y.W., Huang J.-H., Yu G.-P. et al.* // Thin Solid Films 2010. V. 518. P. 7308–7311.
5. *Zywitzki O., Klostermann H., Fietzke F. et al.* // Surf. Coat. Technol. 2006. V. 200. P. 6522–6526.
6. *Holec D., Rachbauer R., Chen Li, et al.* // Surf. Coat. Technol. 2011. V. 200. P. 1698–1704.
7. *Saladukhin I.A., Abadias G., Michel A. et al.* // Thin Solid Films. 2013. V. 538 P. 32–41.
8. *Abadias G., Saladukhin I.A., Uglov V.V. et al.* // Surf. Coat. Technol. 2013. V. 237 P. 187–195.